

Creep- and fatigue-resistant, rapid piezoresistive responses of elastomeric graphene-coated carbon nanotube aerogels over wide pressure range

Michelle N. Tsui and Mohammad F. Islam*

Department of Materials Science and Engineering, Carnegie Mellon University, 5000 Forbes Avenue, Pittsburgh, PA 15213, USA. E-mail: mohammad@cmu.edu

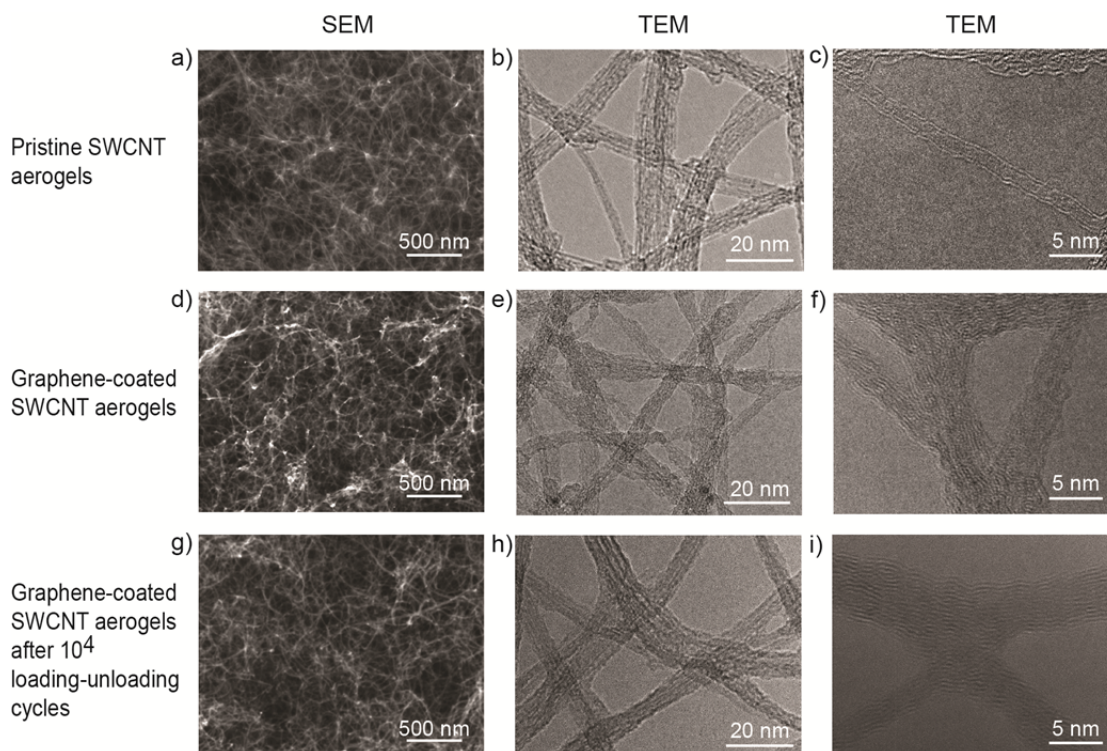


Fig. S1. Microstructure of graphene-coated SWCNT aerogels using SEM and TEM imaging of aerogel cross-sections before and after 10^4 loading-unloading cycles to $\sigma = 80$ kPa. a) SEM and b–c) TEM images of pristine SWCNT aerogel. d) SEM and e–f) TEM images of graphene-coated SWCNT aerogels before compression. Both pristine and graphene-coated aerogels are comprised of isotropic networks of pristine SWCNT and graphene-coated SWCNTs, respectively. Based on at least 10 TEM images, the graphene coating on the underlying SWCNT aerogels is non-uniform with most of the junctions between SWCNTs and a fraction of SWCNT struts being coated with graphene. g) SEM and h–i) TEM images of graphene-coated SWCNT aerogels after compressive loading-unloading cycles confirm that the microstructure is preserved.

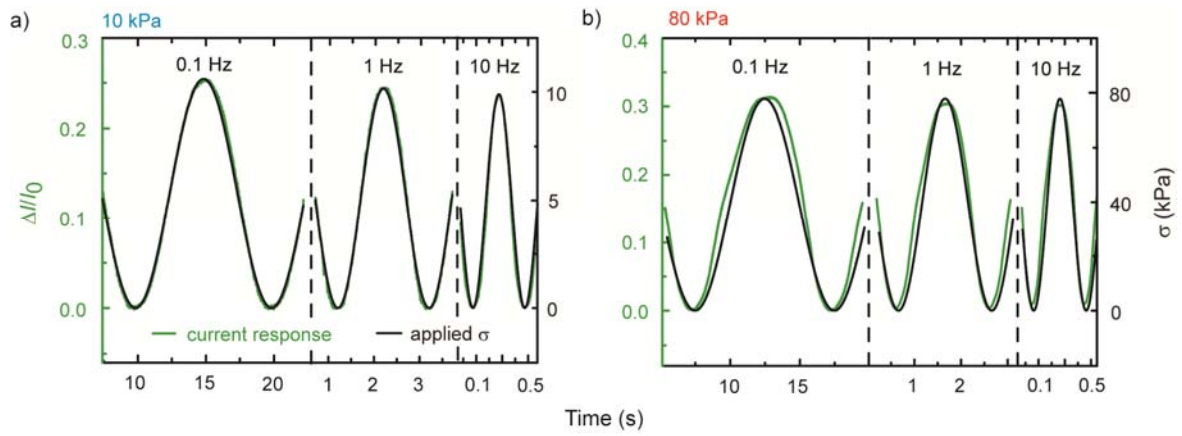


Fig. S2. Determination of the delay time of the piezoresistive properties by overlaying current responses from sinusoidal applied σ of a) 10 kPa peak-to-peak and b) 80 kPa peak-to-peak at frequencies of 0.1 Hz, 1 Hz and 10 Hz.

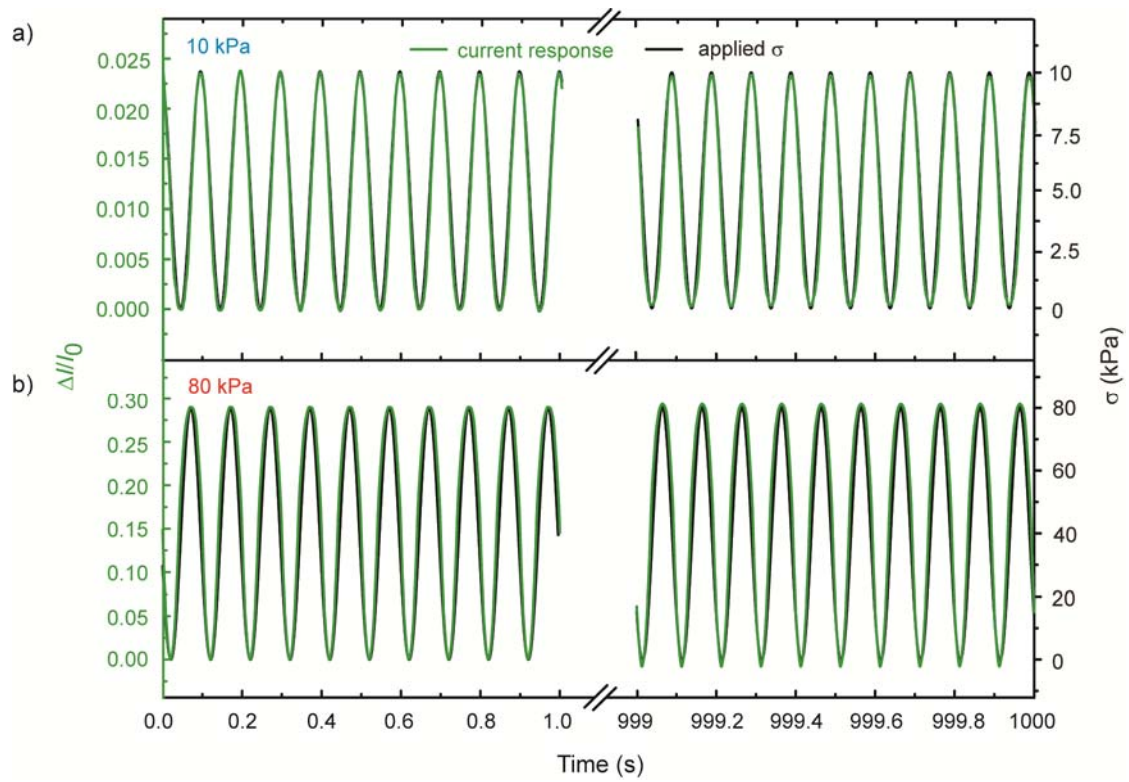


Fig. S3. Overlaying sinusoidal current response corresponding to sinusoidal applied σ for the first and the 1000th second at a loading-unloading cycling frequency of 10 Hz for both a) low (10 kPa peak-to-peak) and b) high (80 kPa peak-to-peak) σ , corroborating fatigue resistance of the piezoresistivity of graphene-coated SWCNT aerogels.

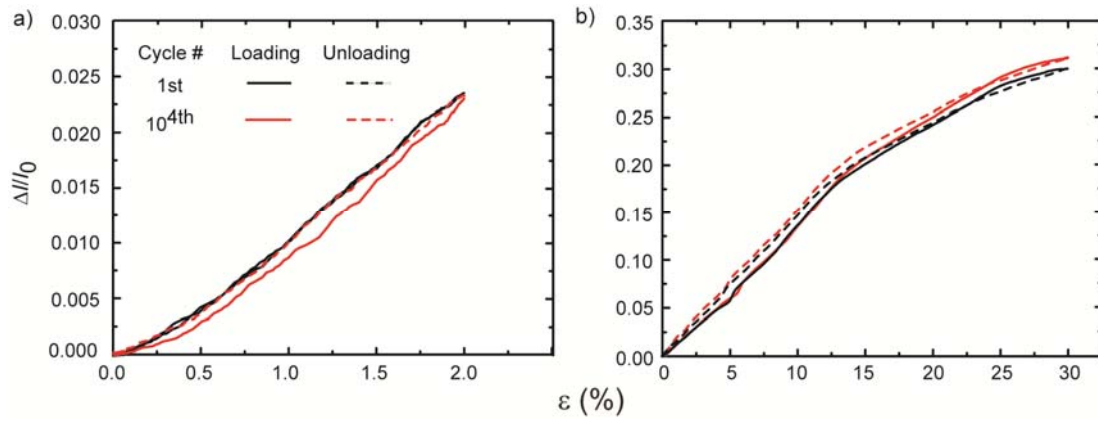


Fig. S4. The current response from the 1st loading-unloading cycle is nearly identical to the current response from the 10⁴th loading-unloading cycle at a frequency of 10 Hz for a) $\epsilon \leq 2\%$ (corresponding $\sigma = 10$ kPa) and b) $\epsilon \leq 30\%$ (corresponding $\sigma = 80$ kPa), again demonstrating fatigue resistance of the piezoresistive responses of graphene-coated SWCNT aerogels.

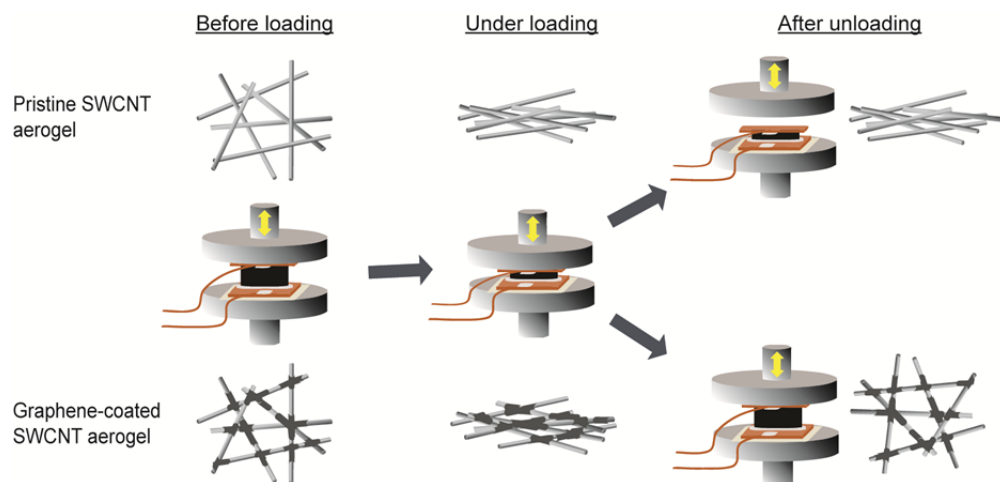


Fig. S5. Schematic illustration of the possible deformation processes of pristine SWCNT aerogels and graphene-coated SWCNT aerogels before loading, under loading and after unloading. Graphene coats mostly the nodes and some of the struts in the graphene-coated SWCNT aerogels, and provides a restoring force for rotation about the junctions and breaking of junctions that formed under loading. This allows recovery of graphene-coated SWCNT network to pre-loading configuration. In contrast, there is no restoring force in pristine SWCNT aerogels to overcome junctions that formed under loading, leading to irreversible deformation.

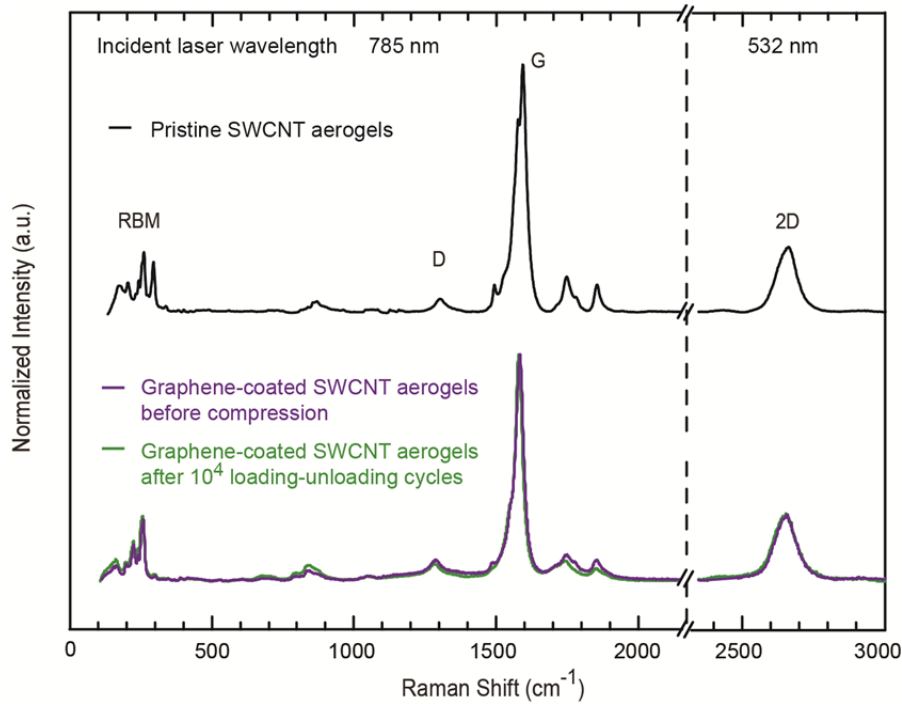


Fig. S6. Raman spectra from pristine SWCNT aerogels, and graphene-coated SWCNT aerogels. The spectra characterize the structural integrity of SWCNTs through the graphene coating process and 10^4 loading-unloading cycles to $\sigma = 80$ kPa as well as the quality of the graphene coating before and after repeated mechanical deformations. The spectra were collected using 785 and 532 nm lasers. The Raman spectra from graphene-coated SWCNT aerogels before and after compression display distinct features associated with SWCNTs and graphene. The Raman intensity ratio I_D/I_G between the SWCNT D-band at ≈ 1300 cm^{-1} and the G-band at ≈ 1590 cm^{-1} of graphene-coated SWCNT aerogels relative to pristine SWCNT aerogels indicates damage or structural defects in SWCNTs from graphene coating.¹ Note, G-band represents sp^2 -hybridized carbon and the D-band quantifies sp^3 -hybridized carbons in the aerogels. The I_D/I_G for graphene-coated SWCNT aerogels increases only slightly to 0.10 from 0.07 for SWCNT aerogels, indicating only minimal damage to SWCNTs from graphene coating. Furthermore, the measurements also confirm that the carbon was indeed graphene and not amorphous carbon. Otherwise, I_D/I_G would have increased after coating. Moreover, the Raman spectra display radial breathing modes (RBMs), which are exclusive features of SWCNTs,¹ corroborating that the SWCNTs remain intact in these graphene-coated SWCNT aerogels. We attribute a slight reduction and a red-shift in peak locations to interactions between SWCNTs and graphene.² The 2D peak, more resonant with 532 nm laser, minimally broadens after graphene coating,³ likely because the amount of graphene in the final aerogels is small. Finally, the Raman spectra from graphene-coated SWCNT aerogels after 10^4 loading-unloading cycles to $\sigma = 80$ kPa is nearly identical to that before compression, validating no structural changes in SWCNTs and graphene during repeated mechanical deformations.

Table S1. Comparison of piezoresistive characteristics of various piezoresistive materials.

Piezoresistive materials	Low pressure S (kPa ⁻¹)	Low pressure range (kPa)	High pressure S (kPa ⁻¹)	High pressure range (kPa)	Response/relaxation time, frequency range	Piezoresistivity creep rate, creep duration, applied pressure	Fatigue of piezoresistivity, ^a loading-unloading cycles, ε (corresponding σ)	Ref.
Graphene-coated SWCNT aerogels	0.0024–0.0069	<30	0.0032	30–120	<27 ms, 1–10 Hz	$\approx 0 \text{ s}^{-1}$, 1 hr, 80 kPa	≈ 0 , 10^4 , 35% (80 kPa)	This work
MWCNT/PDMS microdome ^b	15.1	≤ 0.5	0.0001	0.5–10	40 ms, 0.125 Hz	N.A. ^c	$\approx 5\%$, 10^3 , 4–5% (58.8 kPa)	4
Gold nanowire	1.14	≤ 5	N.A. ^c	50	17–50 ms, 1–5.5 Hz	N.A. ^c	$\approx 14\%$, 10^4 , N.A. ^c (3 kPa)	5
RGO/PU foam ^d	0.26	≤ 2	0.03	2–10	N.A. ^c	N.A. ^c	≈ 0 , 5×10^4 , N.A. ^c (2 kPa)	6
Graphene foam	0.23–10	0.082–2.75	N.A. ^c	N.A. ^c	5–700 ms, 0.1–10 Hz	0.0013 s^{-1} , 10 s, 87 kPa	≈ 0 , 10^4 , 10% (1 kPa)	7
Laser-scribed graphene	0.96	≤ 50	N.A. ^c	50–113	0.4–212 ms, 0.25–0.5 Hz	0.0236 s^{-1} , 0.5 s, 72 kPa	≈ 0 , 10^2 , N.A. ^c (75 kPa)	8

^aFatigue of piezoresistivity is quantified as the relative change in $\Delta R/R_0$ or the relative change in $\Delta I/I_0$ after a specified number of loading-unloading cycles to a particular ε or σ .

^bMWCNT \equiv multiwalled carbon nanotube.

^cValues were not reported.

^dRGO \equiv reduced graphene oxide; PU \equiv polyurethane.

References

- 1 M. S. Dresselhaus, A. Jorio and R. Saito, *Annu. Rev. Condens. Matter Phys.*, 2010, **1**, 89-108.
- 2 E. Wilson and M. F. Islam, *ACS Appl. Mater. Interfaces*, 2015, **7**, 5612–5618.
- 3 K. H. Kim, Y. Oh and M. F. Islam, *Nat. Nanotechnol.*, 2012, **7**, 562-566.
- 4 J. Park, Y. Lee, J. Hong, M. Ha, Y. D. Jung, H. Lim, S. Y. Kim and H. Ko, *ACS Nano*, 2014, **8**, 4689-4697.
- 5 S. Gong, W. Schwalb, Y. Wang, Y. Chen, Y. Tang, J. Si, B. Shirinzadeh and W. Cheng, *Nat. Commun.*, 2014, **5**, 1-8.
- 6 H. B. Yao, J. Ge, C. F. Wang, X. Wang, W. Hu, Z. J. Zheng, Y. Ni and S. H. Yu, *Adv. Mater.*, 2013, **25**, 6692-6698.
- 7 L. Qiu, M. Bulut Coskun, Y. Tang, J. Z. Liu, T. Alan, J. Ding, V. T. Truong and D. Li, *Adv. Mater.*, 2016, **28**, 194-200.
- 8 H. Tian, Y. Shu, X. F. Wang, M. A. Mohammad, Z. Bie, Q. Y. Xie, C. Li, W. T. Mi, Y. Yang and T. L. Ren, *Sci. Rep.*, 2015, **5**, 1-6.